Systematical analysis of mode-locked fiber lasers using single-walled carbon nanotube saturable absorbers*

Zhang Xiao(张 晓) and Song Yan-Rong(宋晏蓉)†

Institute of Information Photonics Technology and College of Applied Sciences, Beijing University of Technology, Beijing 100124, *China*

(Received 4 September 2013; revised manuscript received 7 November 2013; published online 10 April 2014)

The output characteristics of the Er-doped mode-locked fiber laser using a single-walled carbon nanotube saturable absorber are investigated theoretically with a nonlinear Schrödinger equation and a saturable absorption equation using realistic parameters. Stable self-starting mode-locking pulses are achieved under net normal, net zero, and net anomalous cavity group velocity dispersion (GVD) respectively. A spectrum with a flat top is obtained from the net normal cavity GVD laser while a spectrum with Kelly side-bands is obtained from the net anomalous cavity GVD laser. The characteristics of the pulse duration changing with cavity GVD and modulation depth of the single-walled carbon nanotubes are discussed. The characteristics of the mode-locking pulses from net normal, net zero, and net anomalous cavity GVD mode-locked fiber lasers are compared. These systematical results are useful for designing mode-locked fiber lasers with saturable absorbers made by different kinds of carbon nano-materials.

Keywords: mode-locked fiber lasers, carbon nanotubes, theory

PACS: 42.60.Fc **DOI:** 10.1088/1674-1056/23/6/064204

1. Introduction

Carbon nanotubes (CNTs), as a cheap, small threshold, broad spectral range mode-locked material, have been extensively studied in recent years.[1–6] In 2002, it was experimentally demonstrated that single-walled carbon nanotubes (SWCNTs) had an exciton decay time of less than 1 ps at 1.5 μm, which revealed that a SWCNT polymer composite may be a candidate material for high-quality sub-picosecond all-optical switches.[7] In 2004, passively mode-locked picosecond fiber lasers in different configurations were demonstrated at 1550 nm using SWCNTs as mode-lockers for the first time.[8] Then, passively mode-locked fiber lasers with SWCNTs operating at 1300 nm,[9] 1064 nm,[10] over a large tuning range ($>$ 50 nm) near 2 μm[11] were presented. In 2008, 115 fs, 39 MHz soliton pulses were successfully generated with an average output power of 3.4 mW by a passively mode-locked fiber laser incorporating a CNTs-doped polycarbonate as a polymer saturable absorber (SA).[12] In 2011, the miniature mode-locked all-fiber Fabry–Pérot lasers (FFPL) by a CNT saturable absorber operation with fundamental repetition rates of 4.24 GHz, 9.63 GHz, and 19.45 GHz were reported.[13] In 2012, an average maximum power of 285 mW and a pulse energy of 8.1 nJ were obtained as the highest values, which have not yet been achieved for single-pulse operation in a nanotube fiber laser.[14] In 2013, mode-locking was achieved with a low threshold pump power of 32 mW in a passively mode-locked Yb-doped fiber laser based on a bandpass filter together with a fabricated novel SWCNT wallpaper absorber.[10] Most of the previous researches have been about the experimental results, but a systematical theoretical analysis has not been presented until now.

In this paper, we theoretically investigate the characteristics of mode-locking in Er-doped fiber lasers using a single-walled carbon nanotube saturable absorber (SWCNT-SA) based on a discrete theoretical model of a nonlinear Schrödinger equation and a saturable absorption equation under realistic parameters. For a complete discussion, three kinds of mode-locking states with net normal, net zero, and net anomalous cavity group velocity dispersion (GVD) are considered. In order to discuss the deciding factors for the pulse durations of mode-locked fiber lasers and the functions of saturable absorbers, a number of mode-locking simulation results are presented according to different net cavity GVDs and different modulation depths.

2. Configuration and model of mode-locked fiber laser

2.1. Configuration of the mode-locked fiber laser using SWCNT-SA

Figure 1 shows an all-fiber Er-doped mode-locked laser using SWCNT-SA. A wavelength-division multiplexer (WDM) and an optical coupler (OC) are used for the input pump light and output laser. To prevent unwanted feedback, an isolator is placed in the cavity. Erbium-doped fiber (EDF) is used as the gain fiber. A PC is a polarization controller. SWCNTs work as a saturable absorber. Changing the length of the

*Project supported by the National Key Basic Research Progrm of China (Grant No. 2013CB922404), the National Natural Science Foundation of China (Grant No. 61177047), and the Key Project of the National Natural Science Foundation of China (Grant No. 61235010).

†Corresponding author. E-mail: yrsong@bjut.edu.cn

© 2014 Chinese Physical Society and IOP Publishing Ltd

erbium-doped gain fiber L_{GF} (normal GVD) and the length of the single mode fiber (SMF) L_{SMF} (anomalous GVD), three different kinds of laser cavities: net normal GVD, net zero GVD, and net anomalous GVD could be realized.

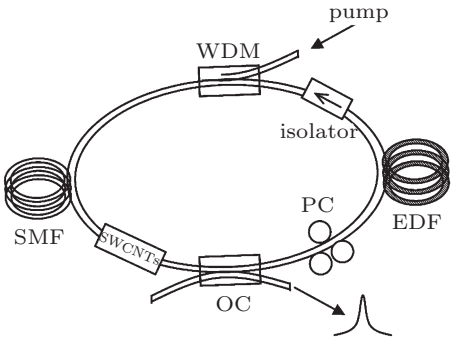


Fig. 1. Configuration of an all-fiber Er-doped mode-locked laser using SWCNT-SA, SMF: single mode fiber, PC: polarization controller, EDF: Er-doped fiber, OC: optical coupler, WDM: wavelength-division multiplexer.

2.2. Model for mode-locked fiber lasers

Here we use a discrete theoretical model of a nonlinear Schrödinger equation and saturable absorption equation to discuss the mode-locked fiber lasers using SWCNT-SA. There are three main components in this model: gain fiber with normal GVD, SMF with anomalous GVD, and SWCNT-SA.

2.2.1. Model for gain fiber and SMF

The gain fiber and SMF are described by the nonlinear Schrödinger equation:[15,16]

$$\frac{\partial A}{\partial z} = -\frac{\mathrm{i}\beta''}{2}\frac{\partial^2 A}{\partial t^2} + \mathrm{i}\gamma|A|^2 A + \frac{g}{2}\left(1+\frac{1}{\Omega_g^2}\frac{\partial^2}{\partial t^2}\right)A - \frac{\alpha}{2}A, \tag{1}$$

where A is the electric field envelope in the fiber; t and z are the time and position along the fiber; β'' is the second order dispersion coefficient and $\beta'' = -\lambda_0^2\bar{D}/(2\pi c)$, with λ_0 being the wavelength and $\lambda_0 = 1.55$ μm, c being the light velocity, $\bar{D} \approx -17$ ps/(km·nm) and 17 ps/(km·nm) for gain fiber and SMF, respectively; γ is the nonlinear coefficient and $\gamma = n_2\omega_0/(cA_{\mathrm{eff}})$. We take $\omega_0 = 2\pi c/\lambda_0$, $n_2 = 2.6\times10^{-16}$ cm^2/W, and $A_{\mathrm{eff}} = 60$ μm^2 for both gain fiber and SMF. The bandwidth of gain $\Omega_g = (2\pi c/\lambda_0^2)\Delta\lambda$ and $\Delta\lambda = 20$ nm. The loss in the fiber is $\alpha = 0.2$ dB/km. It is assumed that a 10% coupling loss occurs at the input and output of each of the different elements. For an SMF, we take the gain g to be 0. For a gain fiber, the gain saturation is described as[17]

$$g = G\cdot\exp\left[-\frac{\int|A|^2\,\mathrm{d}t}{P_{\mathrm{sat}}}\right], \tag{2}$$

where G is the small signal gain coefficient; P_{sat} is the saturation energy and $P_{\mathrm{sat}} = 50$ pJ; $|A|^2$ is the laser power in the fiber.

2.2.2. Model for SWCNT-SA

The total loss of SWCNT-SA is

$$\alpha_{\mathrm{SWCNT}}(t) = \alpha_{\mathrm{c}} + \alpha_{\mathrm{s}}(t), \tag{3}$$

where the inherent loss of SWCNT-SA α_{c} is a constant. The saturable absorption loss of SWCNT-SA $\alpha_{\mathrm{s}}(t)$ is given by[15]

$$\frac{\partial\alpha_{\mathrm{s}}(t)}{\partial t} = \frac{\alpha_0-\alpha_{\mathrm{s}}(t)}{\tau_{\mathrm{s}}} - \frac{|A|^2}{E_{\mathrm{sat}}}\alpha_{\mathrm{s}}(t), \tag{4}$$

where α_0 is the modulation depth of SWCNTs, $|A|^2$ is the power of laser passing through SWCNTs. We take recovery time $\tau_{\mathrm{s}} = 750$ fs and absorber saturation power $E_{\mathrm{sat}} = 5$ pJ.[3] Including the slow response and recovery, equation (4) is accurate both for slow-responding and fast-responding saturable absorbers. Its analytical solution is

$$\begin{aligned}\alpha_{\mathrm{s}}(t) &= \exp\left\{-\int_0^t\left(\frac{1}{\tau_{\mathrm{s}}}+\frac{|A|^2}{E_{\mathrm{sat}}}\right)\mathrm{d}t\right\}\\ &\times\left(\frac{\alpha_0}{\tau_{\mathrm{s}}}\int_0^t\exp\left\{\int_0^t\left(\frac{1}{\tau_{\mathrm{s}}}+\frac{|A|^2}{E_{\mathrm{sat}}}\right)\mathrm{d}t\right\}\mathrm{d}t+\alpha_0\right).\end{aligned} \tag{5}$$

3. Results and discussion

Figure 2 illustrates the variations of absorptivity $\alpha_{\mathrm{SWCNTs}}(t)$ of the SWCNT-SA with time for different values of modulation depth α_0 (0.02, 0.04, 0.06, 0.08), when the same pulse passes through the SWCNT-SA. The peak power of the pulse is 500 W, and the pulse duration is 140 fs. Here $\alpha_0+\alpha_{\mathrm{c}} = 0.6$. From the figure, we can see that on the front edge of the pulse, $\alpha_{\mathrm{SWCNTs}}(t)$ is reduced rapidly, while on the back edge of the pulse, $\alpha_{\mathrm{SWCNTs}}(t)$ returns to 0.6 slowly. The pulse duration is far shorter than the recovery time of SWCNT-SA τ_{s}. Thus, the front edge of the pulse experiences a greater loss than the other parts. Due to the saturable absorption of SWCNTs, the pulse becomes narrower after having passed through every time, which is necessary for mode-locking. The bigger the modulation depth, the narrower the pulse is.

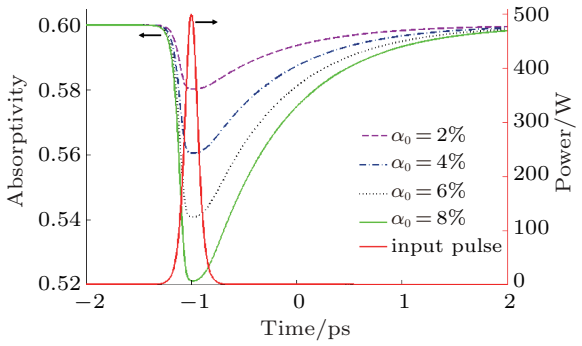


Fig. 2. (color online) Variations of absorptivity of SWCNT-SAs with time for different values of α_0 (0.02, 0.04, 0.06, 0.08), when a temporal pulse passes through the SWCNT-SA.

Because the output characteristics of the mode-locked fiber laser are affected by cavity GVD seriously, three kinds of fiber lasers with net normal, zero or anomalous cavity GVD are discussed using Eqs. (1)–(5). In order to compare the output characteristics of different mode-locked fiber lasers, we set $\alpha_0 = 0.07$ and $\alpha_c = 0.53$ here.

3.1. Net normal cavity GVD mode-locked fiber lasers

Let $L_{GF} = 1$ m and $L_{SMF} = 0.1$ m. The net cavity GVD of the mode-locked laser shown in Fig. 1 is 19530 fs^2. Figure 3(a) demonstrates the time evolution of a stable mode-locked pulse in 1500 round trips in the laser cavity starting from noisy initial conditions when $G = 6$. Due to the temporal compression of SWCNT-SA, the mode-locking takes place from the noise immediately, which is called self-starting. In particular, the front edge of a mode-locked pulse experiences a higher loss than other parts in SWCNT-SA, so that the center of the mode-locked pulse moves to the back side a little after each round trip. The group velocity is a little bit lower than c/n because the mode-locking model used here is based on the group velocity coordinate system. In Fig. 3(b), the absorptivity of SWCNT-SA falls down and recovers according to the laser power in the cavity. A spectrum with a steep edge is very common in experiments with a normal cavity GVD.[18–22] But if the normal cavity GVD and nonlinearity are big enough, a trapezium spectrum will be obtained, just like Fig. 3(c).[23] The full width at half maximum (FWHM) of stable temporal pulse $\Delta\tau$ is 3.6 ps, while the 3-dB bandwidth of spectrum $\Delta\lambda_{3\,\mathrm{dB}}$ is 7.2 nm, which gives a time-bandwidth product ($\Delta\tau\Delta\nu \approx \Delta\tau\Delta\lambda_{3\,\mathrm{dB}}c/\lambda^2$) of 3.2. Therefore the pulses are strongly chirped.

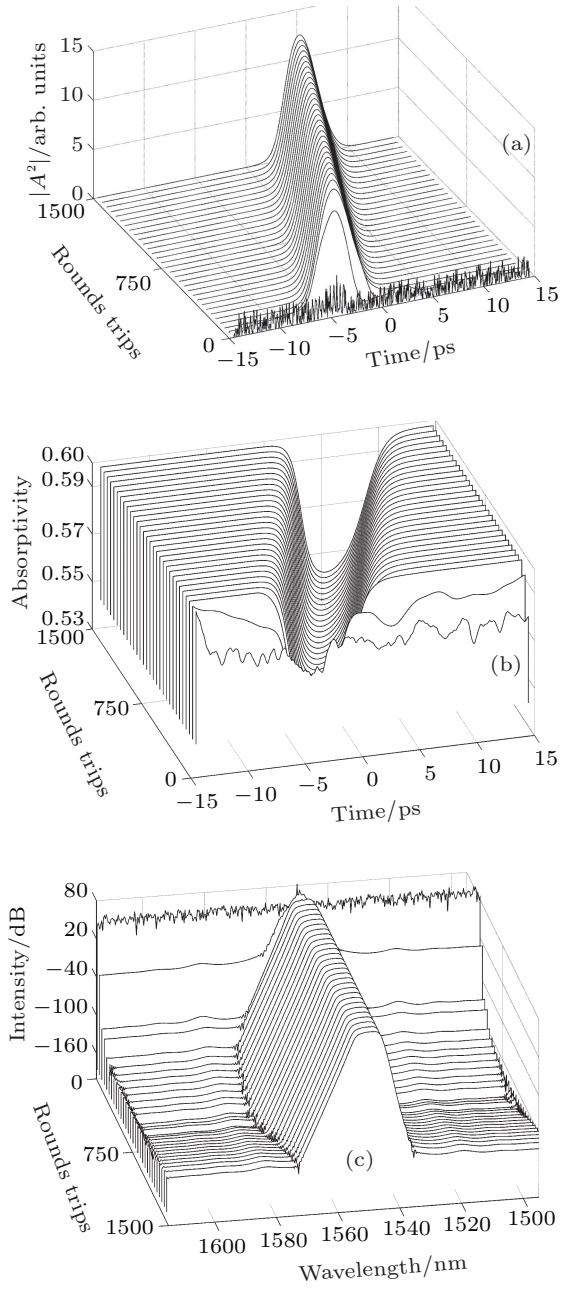


Fig. 3. Self-starting mode-mocking dynamics from the initial noise in the net normal cavity GVD fiber laser using SWCNT-SA: (a) output pulses, (b) absorptivity of SWCNT-SA, (c) spectrum of each round trip.

Figure 4 shows the variation of pulse duration in a round trip after the stable mode-locking state has been reached. Owing to the gain, normal GVD and the nonlinear effect, the pulse duration increases all the time in the gain fiber and reaches a maximum value at the end of the gain fiber. For the dispersion compensation in an SMF, the pulse duration is reduced continuously. Finally, a marked temporal narrowing occurs in the saturable absorber and the pulse duration has a minimum value.

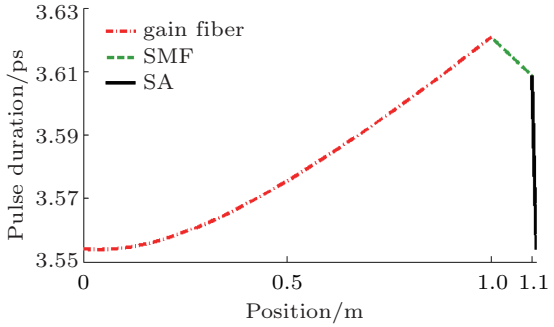


Fig. 4. (color online) Variation of pulse duration with position under a stable mode-locking state in one round trip. Gain fiber (dash–dotted line), SMF (dash line), SA (solid line).

By changing the L_{GF}, the net cavity GVD of a laser could be adjusted. Figure 5 demonstrates the pulse duration, band-width and time-bandwidth product each as a function of net cavity GVD. With the growing of net cavity GVD, the pulse duration increases while the pulse band-width decreases. Meanwhile, the time-bandwidth product rises, which means that the chirp of the pulse increases at the same time.

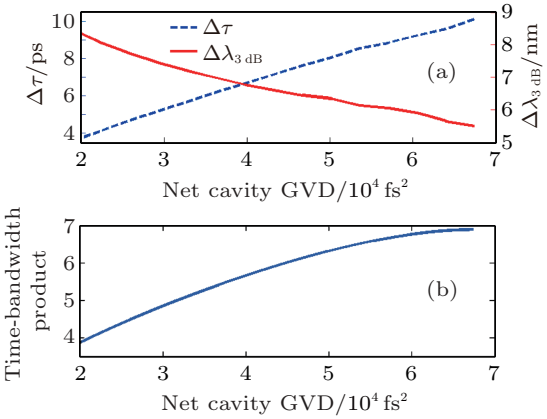


Fig. 5. (color online) Variations of pulse duration and band-width (a) and time-bandwidth product (b) with net cavity GVD.

3.2. Net zero cavity GVD

When $L_{GF} = 1$ m and $L_{SMF} = 1$ m, net cavity GVD of mode-locked laser cavity is zero. Figure 6(a) illustrates the stable self-starting mode-locking in a net zero GVD fiber laser using SWCNT-SA when $G = 1.2$. The front edge of the pulse and the noise floor are attenuated more than the back edge of the pulse when the pulse passes through the saturable absorber. For balance among the GVD, saturable absorption, gain, and nonlinear effect in the cavity, stable mode-locking is obtained after many round trips in the fiber laser cavity. With the same reason as that described in the net normal GVD fiber laser, the group velocity is a little bit lower than c/n. Figure 6(b) shows the absorptivity curves of SWCNT-SA. Figure 6(c) shows the spectra of the net zero GVD mode-locked laser. Compared with the net normal GVD mode-locked laser, the net zero GVD mode-locked laser has spectra each with a sleek and smooth top, which is in accordance with the experiment results.[24,25] With the pulse duration $\Delta\tau = 0.481$ ps and the 3-dB bandwidth of spectrum $\Delta\lambda_{3\,\mathrm{dB}} = 11$ nm, the value of time-bandwidth product is 0.661, which means that the output pulses are rather chirped.

Figure 7 shows the variation of pulse duration with position under stable mode-locking state in a round trip. Although the net GVD of the laser cavity is exactly zero, the pulse duration at the beginning of the gain fiber is smaller than at the end of the SMF. That is because the pulse broadening caused by normal GVD, gain and nonlinear effect in the gain fiber cannot be compressed completely just by anomalous GVD in the SMF. In order to reach the balance between pulse broadening and narrowing, the saturable absorber plays a key role in stable mode-locking. In addition, the functions of the saturable absorber are not only temporally narrowed for pulses but also remove the noise from the cavity.

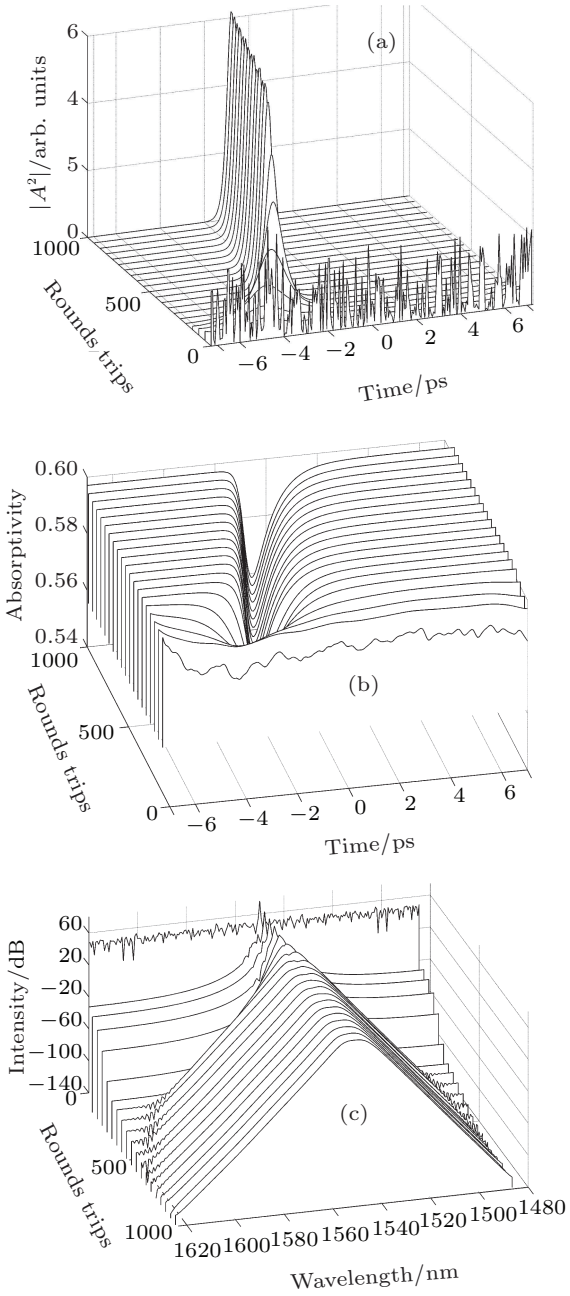


Fig. 6. Self-starting mode-mocking dynamics from the initial noise in the net zero cavity GVD fiber laser using SWCNT-SA: (a) output pulses, (b) absorptivity of SWCNT-SA, (c) spectra every round trip.

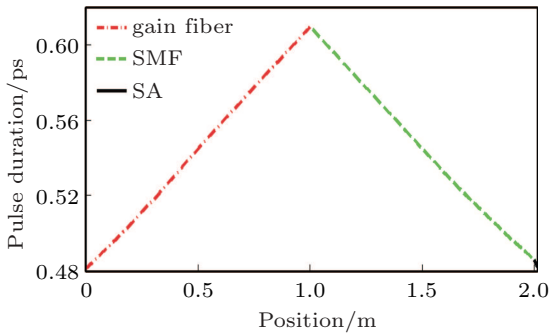


Fig. 7. (color online) Variation of pulse duration with position under stable mode-locking state in a round trip. Gain fiber (dash–dotted line), SMF (dash line), SA (solid line).

3.3. Net anomalous cavity GVD

Let $L_{GF} = 1$ m and $L_{SMF} = 2$ m, then it will give a net cavity GVD of -21700 fs^2. With $G = 1.5$, the self-starting stable mode-locking in net anomalous GVD fiber laser is also obtained in Fig. 8(a). Similarly, the velocity of a mode-locked pulse is a little bit lower than c/n. Figure 8(b) shows the variations of absorptivity of SWCNT-SA with time for each round trip. In Fig. 8(c), spectra with Kelly side-bands are achieved after a steady state has been reached, which shows a similar behavior to the experimental results.[17,26]

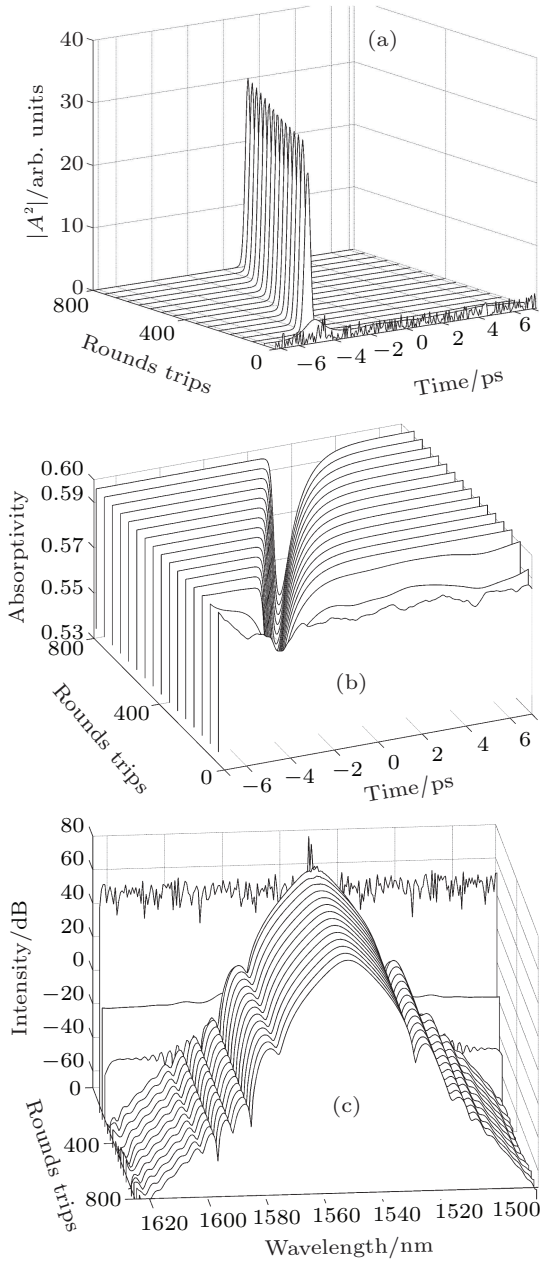


Fig. 8. Self-starting mode-mocking dynamics from the initial noise in the net anomalous cavity GVD fiber laser: (a) output pulses, (b) absorptivity of SWCNT-SA, (c) spectrum every round trip.

The pulse width $\Delta\tau$ (FWHM) of the output mode-locked pulse and 3-dB bandwidth of spectrum $\Delta\lambda_{3\,\mathrm{dB}}$ are 0.351 ps and 9.4 nm respectively. The value of the time-bandwidth product is 0.412. Supposing that the steady state solutions in the net anomalous GVD laser cavity are of a sech^2-type, the pulses are close to the transform-limit, for the time-bandwidth product of the sech^2 function is 0.315.

In Fig. 9, the pulse duration takes the maximum value at the output of the gain fiber. In SMF, the pulse duration decreases and reaches the minimum value. That is a transform-limited state as the chirp caused by normal GVD in the gain fiber is compensated by the anomalous GVD in the SMF completely. Finally, the saturable absorber makes the pulse duration return to the original value.

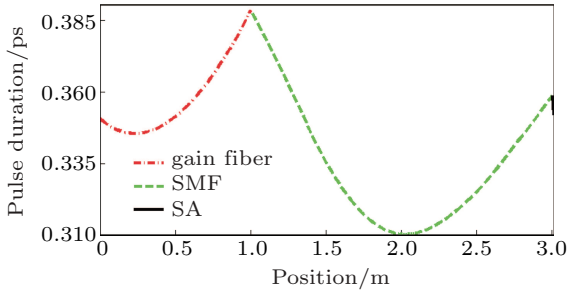


Fig. 9. (color online) Variation of pulse duration with position under the stable mode-locking state in a round trip. Gain fiber (dash–dotted line), SMF (dash line), SA (solid line).

With the increase of the length of SMF L_{SMF}, the value of the net cavity GVD falls, the pulse duration increases and the band-width decreases as shown in Fig. 10. Meanwhile, the time-bandwidth product is reduced and tends to change more and more slowly, for a weakly chirped soliton-like state could be reached in the cavity.

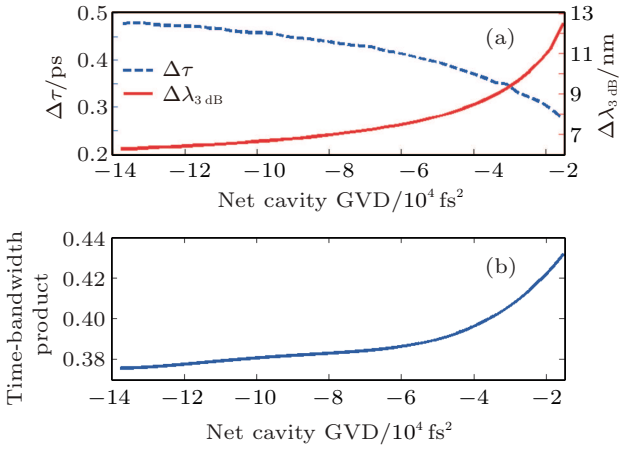


Fig. 10. (color online) Variations of pulse duration and band-width (a) and time-bandwidth product (b) with net cavity GVD.

3.4. Comparision among different net cavity GVD mode-locked fiber lasers using SWCNT-SA

Figure 11 illustrate the transmittances of SWCNT-SA (dash–dotted line, right axes) and the pulse shapes (left axes)

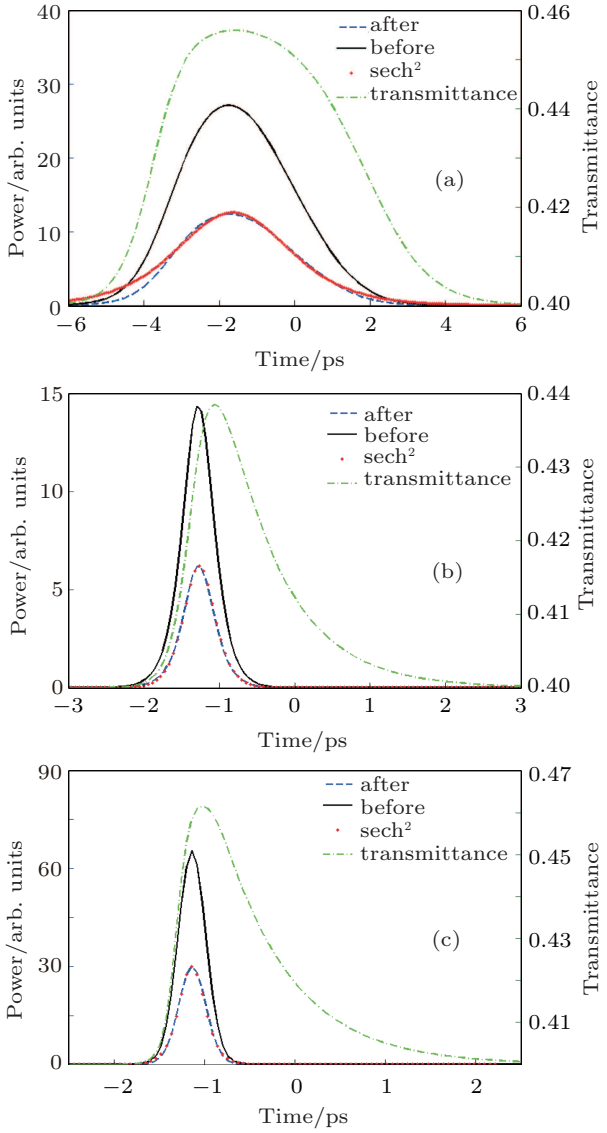


Fig. 11. (color online) Transmittances of SWCNT-SA (dash–dotted line, right axes) and the pulse shapes (left axes) before passing (solid line) and after having passed (dash line) through the saturable absorber under stable mode-locking conditions: (a) net normal cavity GVD, (b) net zero cavity GVD, (c) net anomalous cavity GVD. The dotted line denotes sech^2 fitting curve.

before passing (solid line) and after having passed (dash line) through the saturable absorber under stable mode-locking conditions: (a) net normal cavity GVD, (b) net zero cavity GVD, (c) net anomalous cavity GVD. Corresponding to the three conditions, the output pulse durations are 3.6 ps, 0.481 ps, and 0.351 ps respectively. Figure 11(a) shows the net normal cavity GVD condition. Due to the slow response and recovery of SWCNT-SA, the peak of transmittance appears later than the input pulse peak, thus the front edge of the pulse suffers a greater loss than the back edge. For this reason, the front edge of the output pulse from a net normal cavity GVD laser is lower than the sech^2 function fitting points. Figures 11(b) and 11(c) show the pulses in net zero and anomalous cavity GVD lasers are almost both close to the sech^2 function fitting points. The reason is that the length of the SMF is long enough to force the pulses to form a soliton-like state, which is of a symmetric shape.

Figure 12 demonstrates the output pulse duration $\Delta\tau$ (dash line) and 3-dB bandwidth of output spectrum $\Delta\lambda_{3\,\mathrm{dB}}$ (solid line) versus α_0 under three stable mode-locking conditions in net normal, net zero, and net anomalous cavity GVD mode-locked fiber lasers respectively. The results show that as the modulation depth α_0 increases, the ability to temporally narrow SWCNT-SA increases, pulse duration decreases, and spectral width increases. A comparison of output pulse widths among these three kinds of mode-locked lasers shows that the duration of output pulses from a net normal GVD laser is the biggest while the duration of output pulse from a net anomalous GVD laser is the smallest under the same α_0. The chirp caused by a normal GVD and nonlinear effect leads to the widest output pulse, for these two physical effects cannot balance each other forever. In a net anomalous cavity GVD laser, the scenarios are just the opposite.

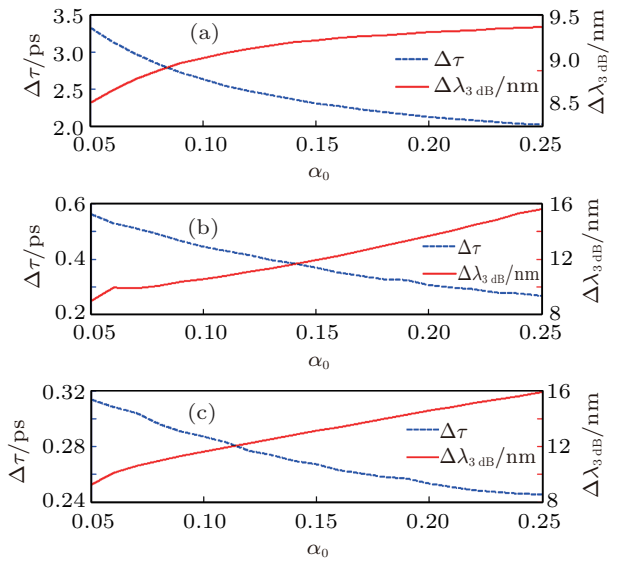


Fig. 12. (color online) Output pulse duration $\Delta\tau$ (dash line) and 3-dB bandwidth of output spectrum $\Delta\lambda_{3\,\mathrm{dB}}$ (solid line) versus α_0 under three stable mode-locking conditions in mode-locked fiber lasers: (a) net normal cavity GVD, (b) net zero cavity GVD, (c) net anomalous cavity GVD.

4. Conclusion

In this paper, simulation results show that stable self-starting mode-locking can be obtained in net normal, net zero, and net anomalous cavity GVD Er-doped fiber lasers using SWCNT-SA. For the net normal cavity GVD laser, the pulse width is broad and the pulse is highly-chirped. The spectrum has a flat top shape. For the net anomalous cavity GVD laser, the pulse width is short and the pulse is nearly transform-limited, which appears to be the shortest in these three kinds of lasers. The spectrum has Kelly side-bands. For both net normal and anomalous GVD mode-locked lasers, as the absolute value of the net cavity GVD grows, the pulse duration

increases and the pulse band-width decreases. However, if the absolute value of the net cavity GVD increases, the time-bandwidth product of pulses from a normal GVD cavity turns greater, while the time-bandwidth product of pulses from an anomalous GVD cavity shows the reverse trend. When increasing the modulation depth of the SWCNT-SA, the ability to temporally narrow SWCNT-SA increases, and the pulse duration of the mode-locked fiber laser decreases.

References

[1] Hernandez-Romano I, Mandridis D, May-Arrioja D A, Sanchez-Mondragon J J and Delfyett P J 2011 *Opt. Lett.* **36** 2122

[2] Baylam I, Ozharar S, Cankaya H, Choi S Y, Kim K, Rotermund F, Griebner U, Petrov V and Sennaroglu A 2012 *Opt. Lett.* **37** 3555

[3] Schmidt A, Rivier S, Steinmeyer G, Yim J H, Cho W B, Lee S, Rotermund F, Pujol M C, Mateos X, Aguiló M, Díaz F, Petrov V and Griebner U 2008 *Opt. Lett.* **33** 729

[4] Hernandez-Romano I, Davila-Rodriguez J, Mandridis D, Sanchez-Mondragon J J, May-Arrioja D and P Delfyett J 2011 *J. Lightwave Technol.* **29** 3237

[5] Zhao G Z, Xiao X S, Meng F, Mei J W and Yang C X 2013 *Chin. Phys. B* **22** 104205

[6] Qu Z S, Wang Y G, Liu J, Zheng L H, Su L B and Xu J 2012 *Chin. Phys. B* **21** 064211

[7] Chen Y C, Raravikar N R, Schadler L S, Ajayan P M, Zhao Y P, Lu T M, Wang G C and Zhang X C 2002 *Appl. Phys. Lett.* **81** 975

[8] Set S Y, Yaguchi H, Tanaka Y and Jablonski M 2004 *J. Lightwave Technol.* **22** 51

[9] Song Y, Set S Y, Yamashita S, Goh C S and Kotake T 2005 *IEEE Photon. Technol. Lett.* **17** 1623

[10] Li X, Wang Y, Wang Y, Liu X, Zhao W, Hu X, Yang Z, Zhang W, Gao C, Shen D, Li C and Tsang Y H 2013 *Opt. Laser Technol.* **47** 144

[11] Fang Q, Kieu K and Peyghambarian N 2010 *IEEE Photon. Technol. Lett.* **22** 1656

[12] Shohda F, Shirato T, Nakazawa M, Komatsu K and Kaino T 2008 *Opt. Express* **16** 21191

[13] Martinez A and Yamashita S 2011 *Opt. Express* **19** 6155

[14] Nozaki Y, Nishizawa N, Omoda E, Kataura H and Sakakibara Y 2012 *Opt. Express* **37** 5079

[15] Agrawal G 2001 *Applications of Nonlinear Fiber Optics* (Scan Diego: Academic Press)

[16] Liu X M, Han D D, Sun Z P, Zeng C, Lu H, Mao D, Cui Y D and Wang F Q 2013 *Sci. Rep.* **3** 2718

[17] Tang D Y, Zhang H, Zhao L M and Wu X 2008 *Phys. Rev. Lett.* **101** 153904

[18] Liu X, Wang L, Li X, Sun H, Lin A, Lu K, Wang Y and Zhao W 2009 *Opt. Express* **17** 8506

[19] Wang R, Dai Y, Yan L, Wu J, Xu K, Li Y and Lin J 2012 *Opt. Express* **20** 6406

[20] Liu X M 2010 *Phys. Rev. A* **81** 023811

[21] Liu X M 2010 *Phys. Rev. A* **82** 063834

[22] Kong L J, Xiao X S and Yang C X 2011 *Chin. Phys. B* **20** 024207

[23] Liu X M 2009 *Opt. Express* **17** 22401

[24] Mao D, Liu X and Lu H 2012 *Opt. Lett.* **37** 2619

[25] Tan S J, Ismail M A, Shahabuddin N S, Ahmad H, Arof H and Harun S W 2012 *Laser Phys.* **22** 1240

[26] Song Y F, Zhang H, Tang D Y and Shen D Y 2012 *Opt. Express* **20** 27283